The Cryosphere, 12, 3877–3890, 2018
https://doi.org/10.5194/tc-12-3877-2018

The Cryosphere Open Access EGU

Variability in individual particle structure and mixing states between the glacier–snowpack and atmosphere in the northeastern Tibetan Plateau

Zhiwen Dong[1,2], Shichang Kang[1,3], Dahe Qin[1], Yaping Shao[2], Sven Ulbrich[2], and Xiang Qin[1,4]

[1]State Key Laboratory of Cryosphere Sciences, Northwest Institute of Eco-Environment and Resources, Chinese Academy of Sciences, Lanzhou 730000, China
[2]Institute for Geophysics and Meteorology, University of Cologne, Cologne 50923, Germany
[3]CAS Center for Excellence in Tibetan Plateau Earth Sciences, Beijing 100101, China
[4]Qilian Shan Station of Glaciology and Ecological Environment, Chinese Academy of Sciences, Lanzhou 730000, China

Correspondence: Zhiwen Dong (dongzhiwen@lzb.ac.cn) and Shichang Kang (shichang.kang@lzb.ac.cn)

Received: 15 August 2018 – Discussion started: 10 September 2018
Revised: 27 November 2018 – Accepted: 2 December 2018 – Published: 13 December 2018

Abstract. Aerosols affect the Earth's temperature and climate by altering the radiative properties of the atmosphere. Changes in the composition, morphological structure, and mixing state of aerosol components will cause significant changes in radiative forcing in the atmosphere. This work focused on the physicochemical properties of light-absorbing particles (LAPs) and their variability through deposition process from the atmosphere to the glacier–snowpack interface based on large-range observations in the northeastern Tibetan Plateau, and laboratory transmission electron microscope (TEM) and energy dispersive X-ray spectrometer (EDX) measurements. The results showed that LAP particle structures changed markedly in the snowpack compared to those in the atmosphere due to black carbon (BC) and organic matter (OM) particle aging and salt-coating condition changes. Considerably more aged BC and OM particles were observed in the glacier and snowpack surfaces than in the atmosphere, as the concentration of aged BC and OM varied in all locations by 4 %–16 % and 12 %–25 % in the atmosphere, whereas they varied by 25 %–36 % and 36 %–48 % in the glacier–snowpack surface. Similarly, the salt-coated particle ratio of LAPs in the snowpack is lower than in the atmosphere. Albedo change contribution in the Miaoergou, Yuzhufeng, and Qiyi glaciers is evaluated using the SNICAR model for glacier surface-distributed impurities. Due to the salt-coating state change, the snow albedo decreased by 16.7 %–33.9 % compared to that in the atmosphere. Such a great change may cause more strongly enhanced radiative heating than previously thought, suggesting that the warming effect from particle structure and mixing change in glacier–snowpack LAPs may have markedly affected the climate on a global scale in terms of direct forcing in the cryosphere.

1 Introduction

Aerosols affect the Earth's temperature and climate by altering the radiative properties of the atmosphere (Jacobson, 2001, 2014; Ward et al., 2018). Snow cover and glaciers in cryospheric regions play an important role in global climate change because of their large areas of distribution on the Earth's surface, especially in the Northern Hemisphere, e.g., in the Alps, the Tibetan Plateau, Northern Hemisphere snowpack and the polar regions. Individual pollutant aerosols, e.g., black carbon (BC, or soot), organic carbon (OC) or organic matter (OM), and mineral dust, deposited on glacier–snowpack surfaces cause enhanced surface heat absorption, acting as light-absorbing particles (LAPs), and they thus impact radiative forcing in the cryosphere. Moreover, changes in the composition, morphological structure, and mixing state of different LAP components will cause significant variability in individual particle radiative heating with largely varied surface albedo due to the changes in a single particle's mixing states (Cappa et al., 2012; Peng et al., 2016).

The Tibetan Plateau, acting as the "third pole" region, is one of the largest cryosphere regions, with an ice mass comparable to the polar regions (Qiu, 2008). Large amounts of LAP particles deposited on the glacier–snowpack surface can significantly impact surface radiative forcing and induce increased heat absorption of the atmosphere in the lower and middle troposphere (Anesio et al., 2009; Kaspari et al., 2011; Dong et al., 2016, 2017), thereby causing rapid glacier melting in the region (Xu et al., 2009; Zhang et al., 2017; Skiles et al., 2018; Dumont et al., 2014).

Aerosols and climate interaction has become a major concern in the Tibetan Plateau region (Dong et al., 2016, 2017). For example, the long-range transport and deposition of BC (soot), various types of salts (e.g., ammonium, nitrate and sulfate), and aerosols, and their climatic significance to the Tibetan Plateau glaciers have recently become heavily researched topics (Ramanathan et al., 2007; Flanner et al., 2007; Zhang et al., 2018). However, to date, notably limited studies have focused on the composition, mixing states, and change processes of LAPs in the atmosphere–snowpack interface of the Tibetan Plateau glacier basins. Moreover, current modeling of the radiative forcing of cryospheric snow and ice, and its impact on climate change has rarely considered influences from changes in the single-particle structure and mixing states (Ramanathan et al., 2007; Hu et al., 2018). Because of glacier ablation and LAP accumulation in summer, the concentration of distributed impurities in glacier–snowpack surface is often even higher than that of the atmosphere (Zhang et al., 2017; Yan et al., 2016).

Therefore, this study aimed to provide a first and unique record of individual LAPs' physicochemical properties, component variability, and mixing states between the glacier–snowpack and atmosphere. It was based on surface-distributed impurity sampling of aerosols (total suspended particle, TSP, on the aerosol filter) and the glacier–snowpack in the northeastern Tibetan Plateau from June 2016 to September 2017 and aimed to determine changes in the structural aging and mixing state of LAPs through atmospheric deposition process from the atmosphere to the glacier–snowpack surface. Thereby it helped to characterize the radiative forcing and climate effects of LAPs in the cryosphere region of the Tibetan Plateau. Moreover, the albedo change contributions of LAPs in several glacier surfaces (e.g., Miaoergou, Yuzhufeng, and Qiyi glaciers) were evaluated using a SNICAR (Single-layer implementation of the Snow, Ice, and Aerosol Radiation) model for the salt mixing states of surface-distributed impurities of the observed glaciers. We organized the paper as follows: in Sect. 2, we provided detailed descriptions on data and methods of individual aerosol particle sampling and analysis, and in Sect. 3 we presented the observed results and discussion of (i) a comparison of LAP components between the atmosphere and glacier–snowpack; (ii) variability in BC/OM particle structure aging between the atmosphere and snowpack; (iii) changes in salt-coating conditions and BC/OM mixing states between the atmosphere and snowpack interface; (iv) variability in particle mixing states and its contribution to radiative forcing. In Sect. 4, we concluded our results and also provided the future study objective for the community.

2 Data and methods

2.1 Field work observation and sampling

The main methods of the study include the fieldwork observations, and laboratory transmission electron microscope (TEM) and energy dispersive X-ray spectrometer (EDX) instrument analysis. Atmospheric LAP samples (TEM aerosol filter samples) and the glacier–snowpack surface-distributed impurity samples were both collected across the northeastern Tibetan Plateau region in summer between June 2016 and September 2017. Figure 1 shows the sampling locations and their spatial distribution in the region, including locations in the eastern Tianshan Mountains, the Qilian Mountains, the Kunlun Mountains, and the Hengduan Mountains, where large-range spatial scale observations were conducted (see Table 1). During the fieldwork sampling, we used the middle volume sampler (DKL-2 (Dankeli) with a flow rate of $150\,\mathrm{L\,min^{-1}}$) for TEM filter sampling in this study, with a flow rate of $1\,\mathrm{L\,min^{-1}}$ for TSP filter sampling in our study, using a single-stage cascade impactor with a 0.5 mm diameter jet nozzle and an airflow rate of $1.0\,\mathrm{L\,min^{-1}}$. Each sample was collected with 1 h duration. After collection, the sample was placed in a sealed dry plastic tube and stored in a desiccator at 25 °C and 20 ± 3 % RH to minimize exposure to ambient air before analysis, and particle smaller than 0.5 mm can be collected efficiently by the instruments. In total, 80 aerosol samples were collected directly on the calcium-coated carbon (Ca-C) grid filter. Additionally, 88 glacier–snowpack surface-snow samples were collected on the glacier–snowpack surface (with 5 cm snow depth, each sampled for 200 mL) for comparison with the deposition process, and the snow samples are taken at the same time of the atmospheric aerosol sampling. The aerosol–snow sampling method is also the same as the previous study in Dong et al. (2016, 2017). The detailed information on sampling locations, time period, and aerosol–snow sample number are shown in Table 1. Snow samples were collected at different elevations along the glacier–snowpack surfaces of the study. Pre-cleaned low-density polyethylene (LDPE) bottles (Thermo Scientific), a stainless steel shovel, and super-clean clothes were used for the glacier–snowpack surface-snow sample collection. All samples were kept frozen until they were transported to the lab for analysis.

2.2 TEM–EDX microscopy measurements

Laboratory TEM–EDX measurements were performed directly on the Ca-C filters grids (Dong et al., 2016). Ca-C grids were used as filters with the advantage of clear

Table 1. Sampling locations, sampling dates, and cryoconite-snow depth at mountain glaciers of snowpack the northeastern Tibetan Plateau.

Site	Glacier	Mountains	Locations	Altitude (m a.s.l.)	Sampling date	Number of snow/ aerosols	particles calculated
MG	Miaoergou Glacier	Tianshan Mountains	42.59° N, 94.16° E	3800–4200	12–13 June 2017	8/8	> 1200
LG12	Laohugou Glacier no. 12	Qilian Mountains	39.20° N, 96.34° E	4300–4700	10–25 July 2016, 3–8 June, 10–21 August 2017	20/24	> 1200
QG	Qiyi Glacier	Qilian Mountains	39.14° N, 97.45° E	4200–4750	10–12 June 2017, 20–22 August 2017	11/8	> 1200
DS	Daban Snowpack	Daban Mountains	37.21° N, 101.24° E	3500–3700	3–4 June 2017	8/4	> 1200
LG	Lenglongling Glacier	Qilian Mountains	37.51° N, 101.54° E	3558–3990	5–7 June 2017	12/5	> 1200
SG	Shiyi Glacier	Qilian Mountains	38.21° N, 99.88° E	3900–4400	3–4 June 2017	9/6	> 1200
YG	Yuzhufeng Glacier	Kunlun Mountains	35.41° N, 94.16° E	4300–4720	12 June 2017	12/11	> 1200
GS	Gannan Snowpack	Gannan Plateau	34.2° N, 103.5° E	2900–3200	4–8 May 2017, 6–9 August 2017	6/6	> 1200
DG	Dagu Glacier	Hengduan Mountains	33° N, 101° E	3200–3900	20–22 September 2017	2/3	> 1200
HG	Hailuogou Glacier	Hengduan Mountains	31° N, 101° E	2900–3500	11–12 August 2017	6/4	> 1200

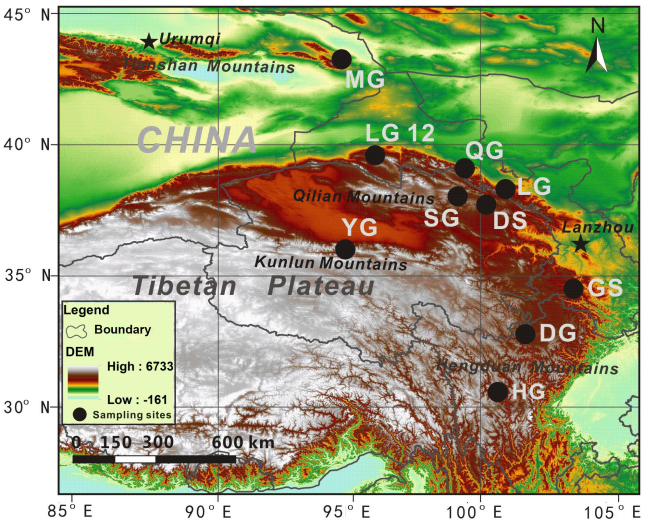

Figure 1. Location map showing the sampled glaciers and snowpack in the northeastern Tibetan Plateau, including the Miaoergou Glacier (MG), Laohugou Glacier no. 12 (LG12), Qiyi Glacier (QG), Lenglongling Glacier (LG), Shiyi Glacier (SG), Dabanshan snowpack (DS), Yuzhufeng Glacier (YG), Gannan Snowpack (GS), Dagu Glacier (DG), and Hailuogou Glacier (HG), where large-range field observations of atmosphere and glacier surface impurities were conducted.

and unprecedented observation for single-particle analyses of aerosols and snowpack samples (Creamean et al., 2013; Li et al., 2014; Semeniuk et al., 2014). Analyses of individual particle observations were conducted using a JEM-2100F (Japan Electron Microscope) transmission electron microscope operated at 200 kV. The analyses involved conventional and high-resolution imaging using bright field mode, electron diffraction (Semeniuk et al., 2014; Li et al., 2014), and energy-dispersive X-ray spectrometry. A qualitative survey of grids was undertaken to assess the size and compositional range of particles and to select areas for more detailed quantitative work that was representative of the entire sample. This selection ensured that, despite the small percentage of particles analyzed quantitatively, our results were consistent with the qualitative survey of the larger particle population on each grid. Quantitative information on size, shape, composition, speciation, mixing state, and physical state was collected for a limited set of stable particles. Some LAPs, including nitrate and ammonium sulfate, though not stable under the electron beam, can be easily detected on EDX at low beam intensity. EDX spectra were collected for 15 s in order to minimize radiation exposure and potential beam damage. All stable particles with sizes 20 nm to 35 µm were analyzed within representative grid mesh squares located near the center of the grid. Grid squares with moderate particle loadings were selected for study to preclude the possibility of overlap or aggregation of particles on the grid after sampling. The use of Ca-C grids resulted in clear and unprecedented

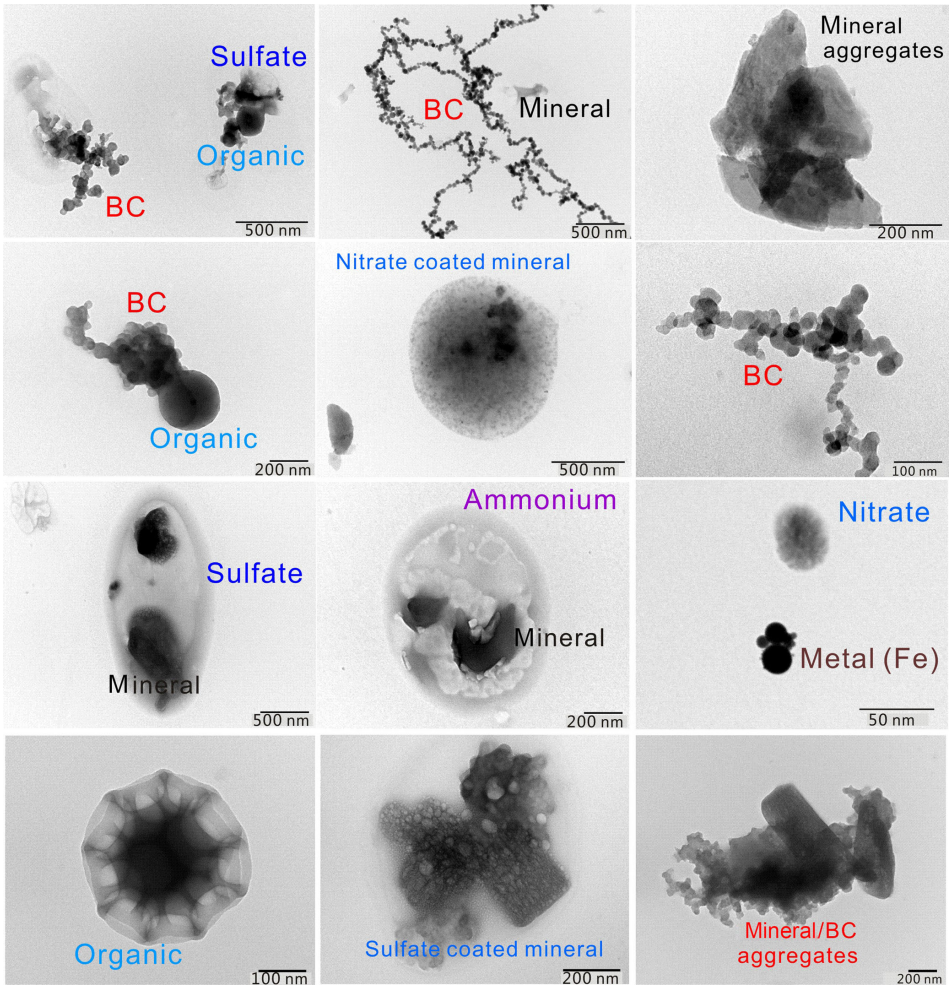

Figure 2. Component types of individual LAP particles in the glaciers and snowpack of the northeastern Tibetan Plateau. Based on the above TEM microscope observation, aerosols were classified into seven type components: NaCl salt, mineral dust, fly ash, black carbon (soot), sulfates, nitrates, and organic matter.

physical and chemical information for the individual particle types. By using TEM–EDX microscope measurements, we can also easily derive the salt-coating conditions based on the advantage of the transmission observation to obtain individual particle inside-structure (Li et al., 2014). Particles (e.g., BC, OM) with salt coating will appear clearly surrounded by various salt shells and with the BC/OM particle as the core. In general, more than 400 particles were analyzed per grid; thus, more than 1200 particles were analyzed from the three grid fractions per sample. Moreover, the snow sample melting will affect individual particle composition during the measurements, especially for various types of salts because the salt is unstable at high temperatures (e.g., ammonium and nitrates) and will change; thus the snow and aerosol samples were directly observed under the TEM instrument and measured before it melted. All samples were measured in frozen states.

2.3 Snow albedo change evaluation

We also simulated the albedo change contributed by the variability of LAPs to individual particle mixing states. The SNICAR model can be used to simulate the albedo of snowpack by a combination of the impurity of the contents (e.g., BC, dust and volcanic ash), snow effective grain size, and incident solar flux parameters (Flanner et al., 2007). In this work, we use the online SNICAR model (http://snow.engin.umich.edu/, last access: 2018). In the SNICAR model, the effective grain sizes of snow were derived from the stratigraphy and ranged from 100 µm for fresh clean snow to 1500 µm for aged snow and granular ice. The model was run with small, medium, and large grain sizes for each snow type to account for the uncertainties in the observed snow grain sizes. Snow density varied with crystal size, shape, and the degree of rimming. The snow density data used in the SNICAR model are summarized with low-, medium-, and high-density sce-

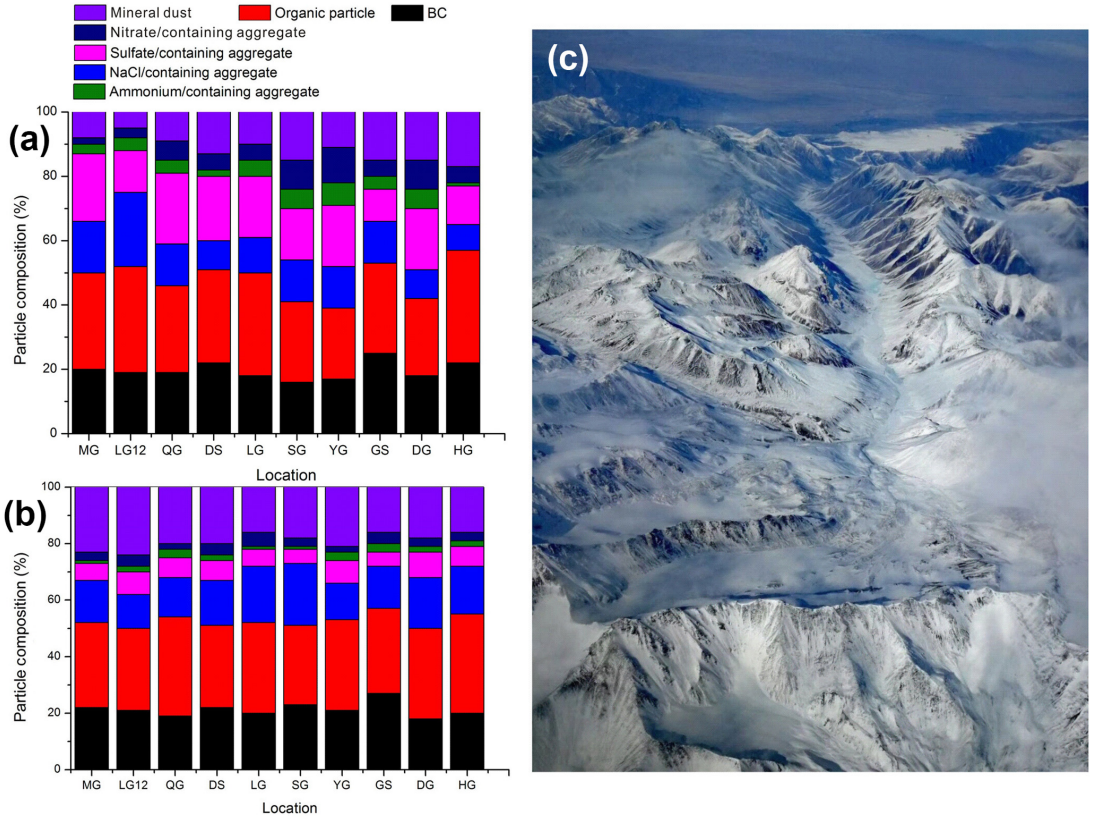

Figure 3. Comparison of individual particle compositions of light-absorbing impurities in the **(a)** atmosphere and **(b)** glacier–snowpack surface in the northeastern Tibetan Plateau, and **(c)** a photo of snowpack and glaciers in the Qilian Mountains taken from a flight in autumn 2017, showing a large distribution of snow cover and glaciers in the northern Tibetan Plateau region.

narios for the model run based on a series of observations in the Tibetan Plateau and previous literature (Judson and Doesken, 2000; Sjögren, 2007;Zhang et al., 2018). In the model simulation, mineral dust ($93.2 \pm 27.05\,\mu g\,g^{-1}$), BC ($1517 \pm 626\,\mu g\,kg^{-1}$) and OC ($974 \pm 197\,\mu g\,kg^{-1}$) average concentration data, as well as other parameters, such as effective grain size, snow density, solar zenith angle, and snow depth on the glaciers, were all considered. The mass absorption cross sections (MACs) for salt-coated BC was referred to the average situation derived from the northern Tibetan Plateau glaciers (Zhang et al., 2017, 2018; Yan et al., 2016; Wang et al., 2013). Although it shows a high level of BC concentration, the data used in this study is comparable to the previous results derived from the Himalaya ice core (Ming et al., 2008), with a relatively higher average elevation on Everest (its deposition site elevation 6500 m a.s.l. compared to 2900–4750 m a.s.l. of northeastern Tibetan Plateau glacier sampling sites) and lower atmospheric BC concentration. Besides, in this work we mainly focus on LAPs (BC, OC, mineral dust, and others) in the glaciers and snowpacks for the surface-distributed impurities; thus impurity is often accumulated in summer with surface ablation and with higher BC concentration.

When running the SNICAR model, BC/OM was assumed to be coated or non-coated with sulfate (Flanner et al., 2007; Qu et al., 2014) or other salts. The MAC is an input parameter for the SNICAR model; it is commonly assumed to be $7.5\,m^2\,g^{-1}$ at 550 nm for uncoated BC particles (Bond et al., 2013). For salt-coated BC particles, the MAC scaling factor was set to be $1\,m^2\,g^{-1}$, following Qu et al. (2014) and Wang et al. (2015). Other impurities (such as volcanic ash) were set to zero. In terms of the albedo calculation, the BC and dust radiative forcing (RF) can be obtained by using Eq. (1) (Kaspari et al., 2014; Yang et al., 2015):

$$\mathrm{RF} = \sum_{0.325\,\mu m}^{2.505\,\mu m} E(\lambda,\theta)(\alpha_{(r,\lambda)} - \alpha_{(r,\lambda,\mathrm{imp})})\Delta\lambda, \quad (1)$$

where α is the modeled snow albedo with or without the impurities (imp) of BC and/or dust; E is the spectral irradiance ($W\,m^{-2}$); r is the snow optical grain size (μm); λ is wavelength (μm); and θ is the solar zenith angle for irradiance (°).

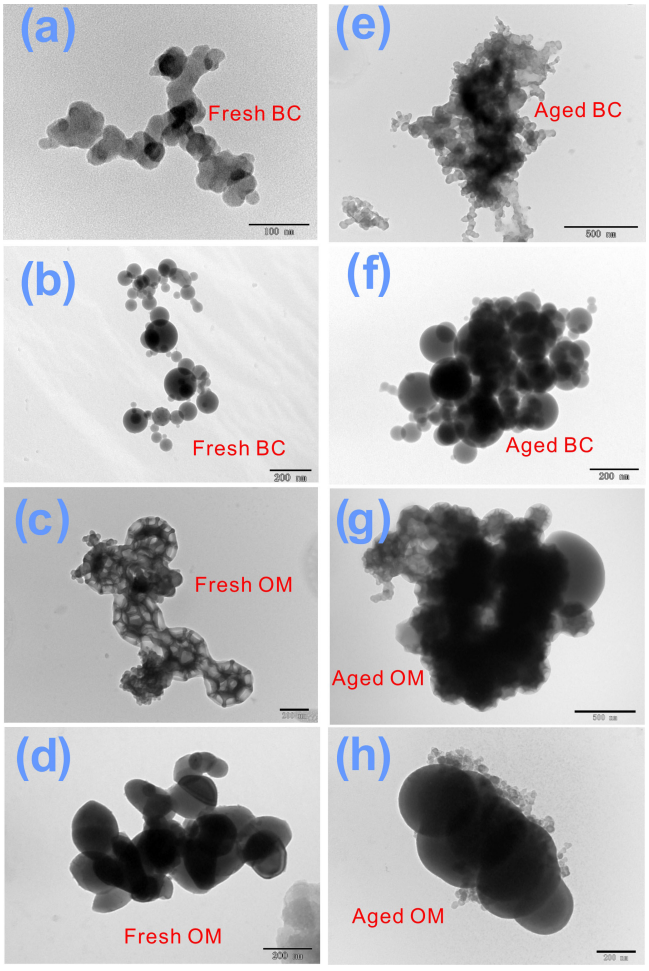

Figure 4. Structural change during the aging of individual black carbon/organic matter particles when deposited from the atmosphere onto snow and ice surfaces. Panels **(a)**–**(d)** represent the atmosphere, while **(e)**–**(h)** show the condition of the glacier–snowpack.

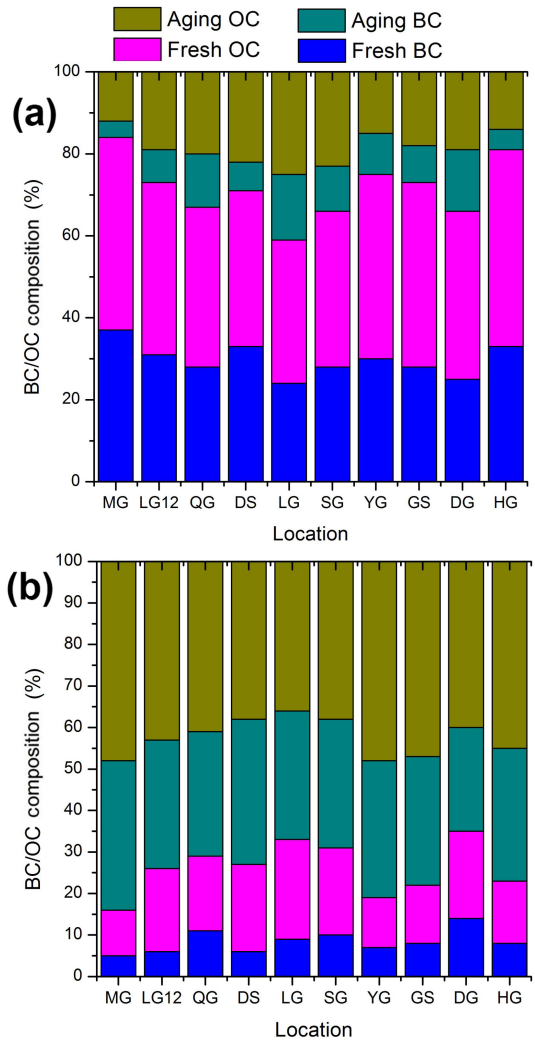

Figure 5. LAP aging of BC/OC individual impurity particles and composition ratio (%) change during the deposition process from the atmosphere to glacier–snowpack. In the figure **(a)** is the atmosphere, and **(b)** is the snowpack.

3 Results and discussion

3.1 Comparison of LAP components between the atmosphere and snowpack

Figure 2 shows the component types of the individual LAPs found in the atmosphere and glacier–snowpack of the northeastern Tibetan Plateau. Based on the above microscope observations, aerosols were classified into seven components: NaCl salt, mineral dust, BC (soot)/fly ash, sulfates, ammonium, nitrates, and organic matter (OM). Classification criteria of sampled particle types, mixing states, and their possible sources in the snow–atmosphere samples were indicated in Table S1 in the Supplement. Figure 3 shows the comparison of individual LAP component types between glacier–snowpack and atmosphere in the northeastern Tibetan Plateau region, which indicates that the LAPs in the atmosphere at various locations are composed of BC (mean percentage of 18.3 %, standard deviation (SD) 2.58), OC (28.2 %, SD 3.49), NaCl (11 %, SD 2.58), sulfate (17 %, SD 3.49); ammonium (4.8 %, SD 3.01), nitrate (7 %, SD 2.83), and mineral dust (13.7 %, SD 3.02), whereas the LAPs in the glacier–snowpack surface are composed of BC (mean 21.3 %, SD 2.49), OC (31.2 %, SD 2.44), NaCl (16.2 %, SD 3.12), sulfate (6.8 %, SD 1.32), ammonium (2 %, SD 0.81), nitrate (3.3 %, SD 0.95), and mineral dust (19.2 %, SD 2.9). We found that the impurity components show large differences between the snowpack and atmosphere in all locations, implying significant change through the aerosol deposition processing in the interface (Fig. 3). LAP components have a large change of proportion in the interface, probably due to different atmospheric cleaning rates and atmo-

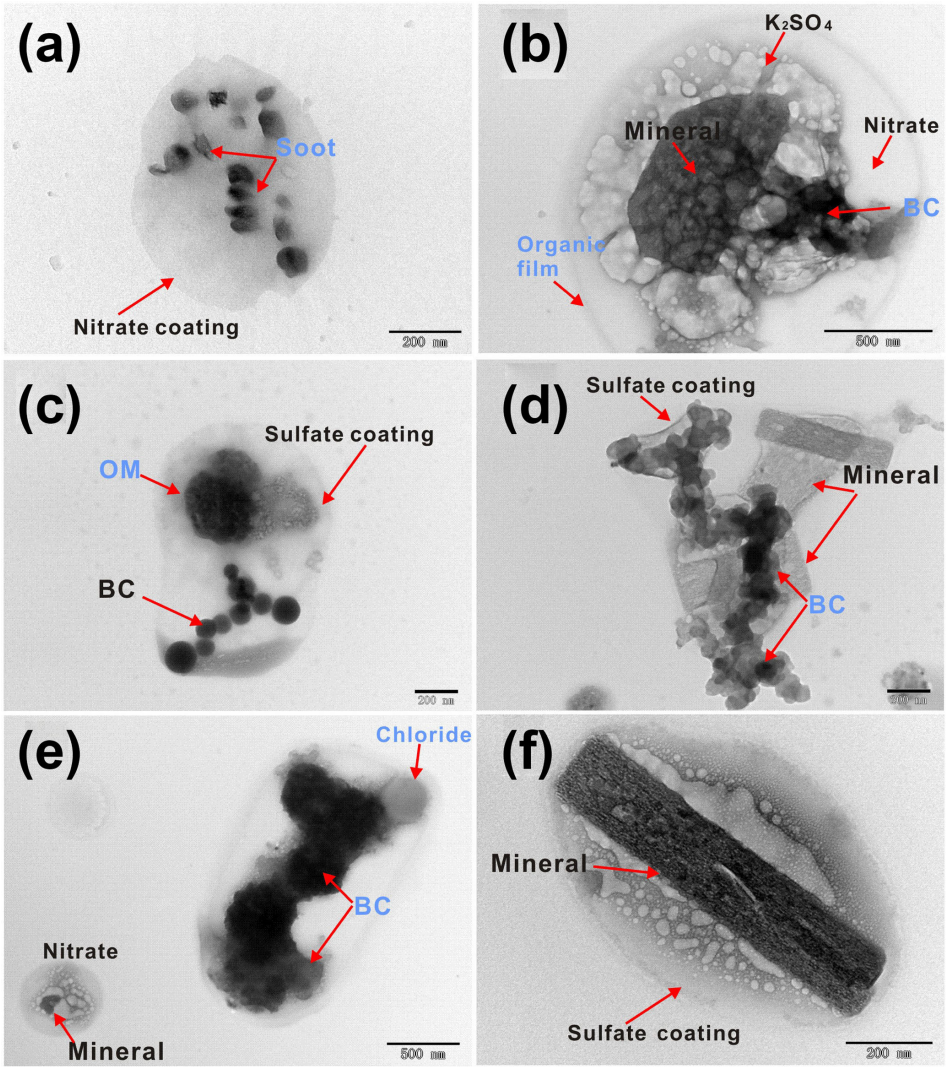

Figure 6. Examples of different salt-coating conditions of BC, OM, and mineral dust for individual particles in the atmosphere from various glacier basins in the northeastern Tibetan Plateau.

spheric processing with dry and wet aerosol deposition. Sulfates and other salts in the atmosphere act as salt-coating forms to other particles with aggregated states and will be dissolved and taken away with precipitating snow and meltwater in the snowpack, which will cause reduced salt components (e.g., sulfate, nitrate, NaCl, and ammonium) in the glacier–snowpack surface compared to those in the atmosphere. Therefore, we can observe obvious changes in composition and mixing states of the impurities between the atmosphere and glacier–snowpack surface in Fig. 3, as the ratio of BC, organic matter, and mineral dust components in the snowpack increased greatly during this process, whereas the ratio of various salts in the snowpack decreased significantly (Fig. 3). The changes in morphology and structure will undoubtedly cause a significant variability in the heat-absorbing property of impurities in both the atmosphere and the glacier–snowpack surface, and these impacts will be discussed in a later section. Moreover, the deposition flux and processing of various types of aerosol particles are different, causing the changes in composition and mixing states of LAP impurities between the atmosphere and cryosphere. Aerosol LAPs change during the atmospheric transport and deposition processes (especially through wet deposition with precipitating snow) will mainly lead to large variability of individual particle's structure and morphology; for example, changes in the aging, salt coating, and mixing state of BC and organic matter (with internal or external mixing), as indicated in following sections, will cause further influences on radiative forcing of the glacier–snowpack surface as discussed in Sect. 3.4.

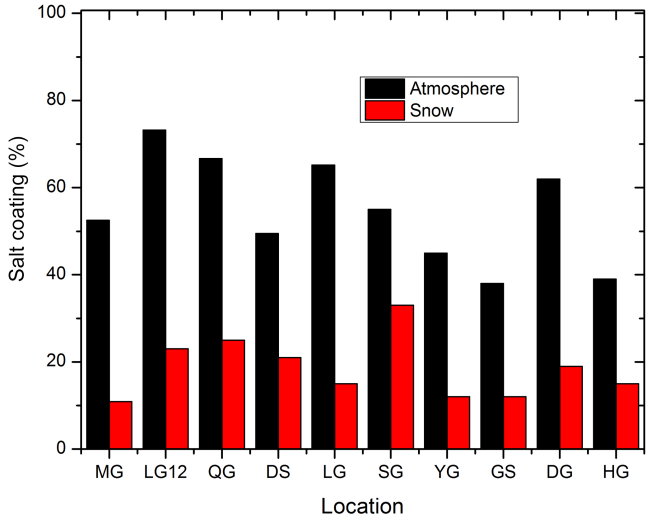

Figure 7. Salt-coating proportion changes of individual impurity particles between glacier–snowpack and atmosphere in various locations of the northeastern Tibetan Plateau.

3.2 BC/OM particle aging between the atmosphere and snowpack

Figure 4 shows how the individual particle's structure changes during the aging process when deposited from the atmosphere onto the glacier–snowpack surface. Figure 4a–d is representative of particles of fresh BC/OM with fractal morphology and a large quantity in the atmosphere, whereas Fig. 4e–h is representative of particles of aged BC/OM with aggregated spherical morphology in the glacier–snowpack surface. It is clear that abundant aerosol particles were observed with a relatively fresh structure in the atmosphere, similarly to previous studies (e.g., Li et al., 2015; Peng et al., 2016). As shown in Fig. 4a–d, the fresh aerosol particles of BC and OC (or organic matter, OM) appeared very common in the atmosphere as the main parts, whereas as shown in Fig. 4e–h, more aged particles were found deposited in the glacier–snowpack surface. This process is characterized by the initial transformation from a fractal structure to spherical morphology and the subsequent growth of fully compact particles. Previous work has indicated the structure and mass absorption cross (MAC) section change of BC particles in the atmosphere (Peng et al., 2016; Yan et al., 2016) but did not discuss such a change in OM particles during the structure-aging process. This study clearly reveals the structural and morphological change in aging BC and OM particles through the transport and deposition processes to the glacier–snowpack from the atmosphere (Fig. 4).

Based on TEM–EDX observations, we evaluated the aged BC/OM particle composition ratio (%) in the snowpack and the atmosphere. Figure 5 shows the aging of BC/OM individual particles and their composition ratio (%) change with the deposition process from the atmosphere to the glacier–snowpack surface. Figure 5 indicates that in the atmosphere the composition ratio is composed of fresh BC (mean percentage of 29.7 %, with SD 3.95), fresh OC (41.8 %, 4.34), aged BC (9.8 %, 4.02), and aged OC (18.7 %, 4.11), while in the snow the composition is fresh BC (mean percentage of 8.4 %, SD 2.71), fresh OC (17.7 %, 4.42), aged BC (31.5 %, 2.99), and aged OC (42.4 %, 4.45). The proportions of aged BC and OM particles varied from 4 % to 16 % and 12 % to 25 % in the atmosphere and from 25 % to 36 % and 36 % to 48 % in the glacier–snowpack surface, respectively. The number of aged particles in snowpack is 2–3 times higher than that in the atmosphere. In the atmosphere, the BC/OM both showed high ratios of fresh structure particles (fractal morphology), while in the glacier–snowpack surface more particles indicated aged structure (spherical morphology), although there was a small portion of particles that were still fresh (Fig. 5). The change in proportion of BC/OM particle aging is very marked between the snow and the atmosphere. The particle structure is a very important factor that influences LAPs (Peng et al., 2016); thus, such changes in BC/OM particles' structure aging between the glacier–snowpack and atmosphere will actually influence the total heat-absorbing property of the mountain glacier–snowpack, even affecting that of the whole cryosphere on the Earth's surface.

3.3 Changes in salt-coating conditions and BC/OM mixing states

In addition to particle structure aging, we find evident variability in particle salt-coating conditions between the atmosphere and the glacier–snowpack interface during the observation period (Fig. 6). Figure 6 demonstrates the different salt-coating examples for individual aerosol particles (including BC, OM, and mineral dust) in the atmosphere in various glacier basins in the northeastern Tibetan Plateau. We found that the salt-coating form is very common for impurity particles in the atmosphere, which will, of course, cause a significant influence on radiative forcing of the atmosphere. A large part of fresh BC/OM (with fractal morphology) and mineral dust particles were coated with various salts, such as sulfate, nitrates, and ammonium. Such obvious salt-coating conditions will cause reduced atmospheric radiative forcing, due to the increase in albedo (IPCC, 2013).

Similarly, we also evaluated the salt-coated particle ratio for BC/OM and its change between the glacier–snowpack and atmosphere (Fig. 7). Figure 7 shows the salt-coating proportion of impurity particles and its difference between the glacier–snowpack interface and atmosphere at those locations. In Fig. 7, the salt-coated particles in the atmosphere accounted for a mean ratio of 54.61 % (with SD 12.02) in various locations, while that in the snow of the glacier–snowpack was 18.59 % (with SD 7.04). The proportion of salt-coating particles varied largely from the atmosphere to the glacier–snowpack surface (2–4 times more in the atmosphere than

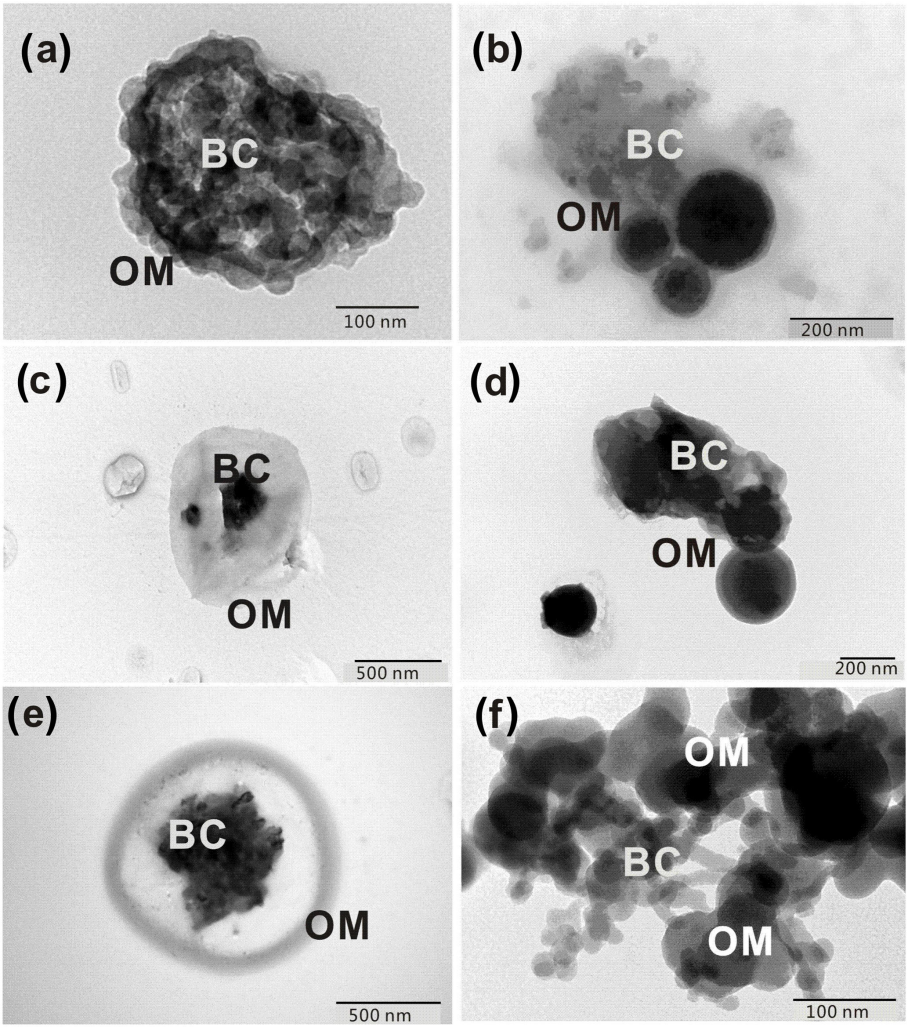

Figure 8. Internal mixing states of BC (soot) and OM in glacier–snowpack in the northeastern Tibetan Plateau in summer 2016–2017.

that in snow). The change proportion of salt-coating particles is very marked, and this change will cause very complicated changes in a particle's mixing states and structure.

Figure 8 shows the situation of internal mixing states of BC (soot), organic matter (OM), and mineral dust particles in various glacier–snowpack in the region, which demonstrates the influence of the transport and deposition process to a particle's structural change. Most salts in the salt-coated particles will disappear when deposited into the glacier–snowpack surface, and the mixing states change largely to the internal and external mixing forms with BC/OM as the core. The proportion change of an internally mixed BC particle with other particles is presented in Fig. 9, showing great increases in internal mixing after deposition among the locations in the whole of the northeastern Tibetan Plateau region. As shown in Fig. 9, the internally mixed particles of BC in the atmosphere accounted for mean ratio 4.68 % (with SD 3.07) in various locations, whereas that in the snow of glacier–snowpack was 14.85 % (with SD 4.93). We find that with the salt-dissolution, a large part of LAPs changed to the internally mixed BC/OM particle with other aerosol particles. As a large number of particles lose their salt coating in the snowpack compared with those in the atmosphere, the whole process will certainly increase the heating absorption proportion of the LAPs. Moreover, as shown in Fig. 10, average conditions of single internally and externally mixed BC/OM individual particles in the glacier–snowpack of the northeastern Tibetan Plateau changed greatly with the diameter of the particle. In Fig. 10, the mixing states of BC/OC in the glacier–snowpack of northeastern Tibetan Plateau showed that the internally, single, and externally mixed BC/OC particles accounted for mean ratios of 69.2 % (SD 22.5), 5.35 % (SD 1.72), and 25.95 % (with SD 22.4). With the increase in particle size, most BC/OM particles ($PM > 1\,\mu m$) showed internal mixing conditions, which will influence the RF of the glacier–snowpack.

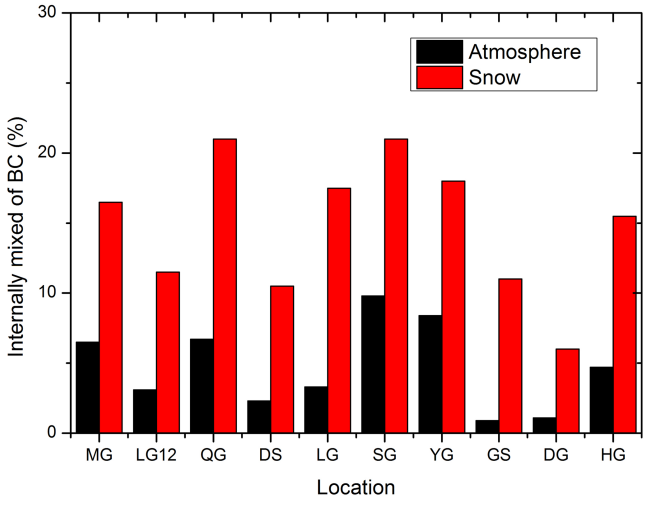

Figure 9. The proportion change of internally mixed BC particle with other particles showing an obvious increase of internally mixed BC/OM in glacier–snowpack compared with that in the atmosphere in summer 2016–2017.

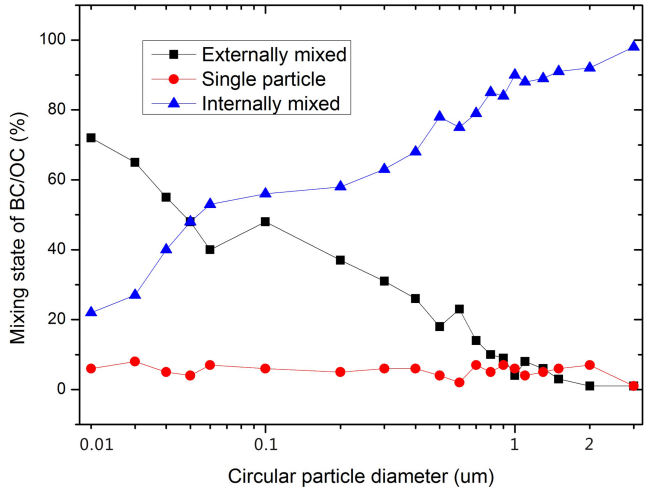

Figure 10. Average conditions of single, internally, and externally mixed BC/OM individual particles in the snowpack of northeastern Tibetan Plateau glaciers, showing most of the BC/OM with diameter $>$ 1 µm in internal mixing conditions.

3.4 Particle mixing state variability and its contribution to light-absorbing properties

Additionally, the extent of influence of LAPs' mixing state changes are also important and need to be evaluated for radiative forcing. The SNICAR model is often employed to simulate the hemispheric albedo of glacier–snowpack for a unique combination of LAP contents (e.g., BC, dust, and volcanic ash), snow effective grain size, and incident solar flux characteristics (Flanner et al., 2007). We also evaluated the influence on albedo change caused by individual particle structure and mixing state changes in the glacier–snowpack of the northeastern Tibetan Plateau region. Figure 11 showed the evaluation of snow albedo changes in BC salt coating in the snowpack compared with that in the atmosphere using SNICAR model simulation in the MG, YG, and QG, showing the albedo change of snow surface impurities in snowpack compared to that of the atmosphere. The parameter input for SNICAR model have been described in the method section. Mineral dust, BC, and OC average concentration data, as well as other parameters, such as effective grain size, snow density, solar zenith angle, and snow depth on the glaciers, and MAC for BC was taken from the average situation in previous work on northern Tibetan Plateau glaciers (Zhang et al., 2017, 2018; Yan et al., 2016; Wang et al., 2013). As shown in Fig. 12, the surface albedo in MG, YG, and QG decreased by 16.7 %–33.9 %, caused by salt-coating changes, when compared to the hypothetical similar situation of impurity composition in the atmosphere. Based on the LAP salt-coating-induced albedo changes, RF was calculated by Eq. (1) for the different scenarios. The results show that the RF change caused by salt-coating changes varied between 1.6 and 26.3 W m^2 depending on the scenario (low, medium, or high snow density).

Figure 12 shows a schematic diagram which explain the particle structure aging and salt-coating changes, and its total influence to the radiative forcing between the atmosphere and glacier–snowpack interface on the northeastern Tibetan Plateau. From the above discussion, we find clear variability in LAP mixing forms between the glacier–snowpack surface and atmosphere, mainly originating from morphological changes in the LAP structure (e.g., aging of BC/OM), and salt-coating changes from increased internal mixing of BC/OC particles, as many particles without salt coating will change to internal mixing with BC/OM particles as a core or to external mixing with BC/OM, which will also significantly influence the total RF of the mountain glacier–snowpack in the cryosphere as indicated in previous work (Jacobson et al., 2001). Moreover, due to glacier ablation and accumulation of various types of impurities, the concentration of impurities in the snowpack surface is often even higher than that of the atmosphere (Zhang et al., 2017; Yan et al., 2016).

In general, as shown in Fig. 12, (i) more fresh BC/OM particles were observed in the atmosphere, whereas more aged BC/OM particles were found on the glacier–snowpack surface. Aged BC/OM particles often mean stronger radiative forcing in the snowpack than in the atmosphere (Peng et al., 2016). (ii) More salt-coated particles were found in the atmosphere of the glacier basin, whereas reduced salt coating was found in the glacier–snow surface. With thick salt coating, the LAP properties may not be that much stronger than the particles without coating, as most salts (sulfate, nitrates, ammonium, and NaCl) did not have strong forcing because of their weak light-absorbing property and high hygroscopicity in the mixing states (IPCC, 2013; Li et al., 2014),

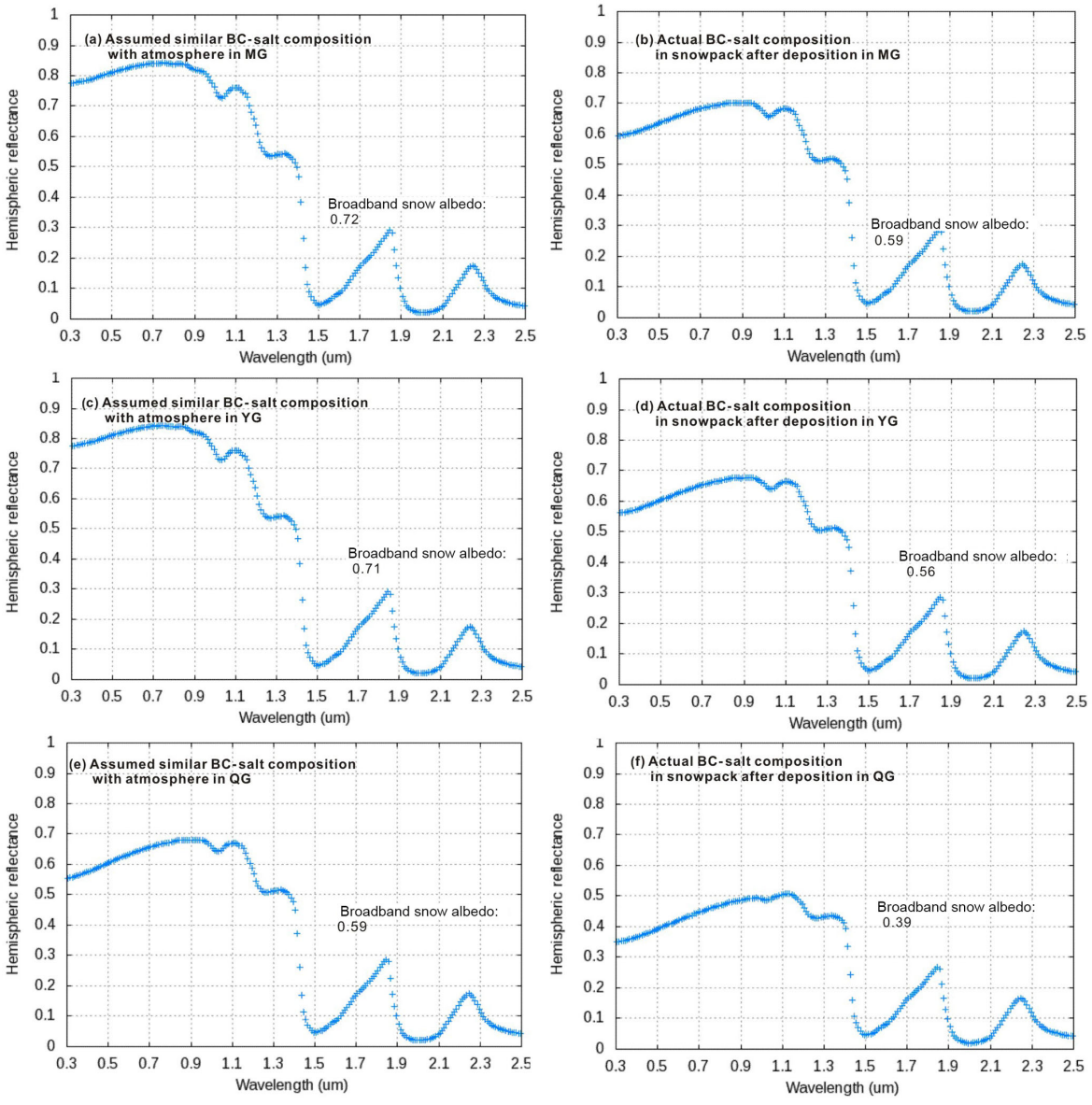

Figure 11. Evaluation of snow albedo change of BC-salt-coating change in the snowpack compared with atmosphere using SNICAR model simulation in the MG **(a, b)**, YG **(c, d)**, QG **(e, f)**, which shows the largely decreased albedo of snow surface impurities in snowpack compared to that of the atmosphere, implying markedly enhanced radiative forcing in the snowpack surface impurities.

especially for sulfate/nitrate aggregated particles. (iii) With the decrease in salt coating, more internally mixed particles of BC/OM surrounded by a well-mixed salt-shell were observed from the individual particles of LAPs in the snow-ice of the cryospheric glacier basin when compared to that of the atmosphere. Internally mixed particles of BC/OM have shown the strongest light absorption in previous modeling studies (Cappa et al., 2012; Jacobson, 2000), as BC acts as a cell-core particle surrounded by organic matter particles (also sometimes including some salts). In a previous study the mixing state was found to affect the BC global direct forcing by a factor of 2.9 ($0.27\,W\,m^{-2}$ for an external mixture, $+0.54\,W\,m^{-2}$ for BC as a coated core, and $+0.78\,W\,m^{-2}$ for BC as well mixed internally) (Jacobson, 2000), and that the mixing state and direct forcing of the black-carbon component approach those of an internal mixture, largely due to coagulation and growth of aerosol particles (Jacobson, 2001), and also found radiative absorption enhancements due to the mixing state of BC as indicated in Cappa et al. (2012) and He et al. (2015). (iv) In addition to the LAPs from the above particle structure change, the absorbing property of some components in the atmosphere and cryosphere (snow and ice) also show large variability, as most mineral and OM (or OC) particles show negative radiative forcing in the atmosphere

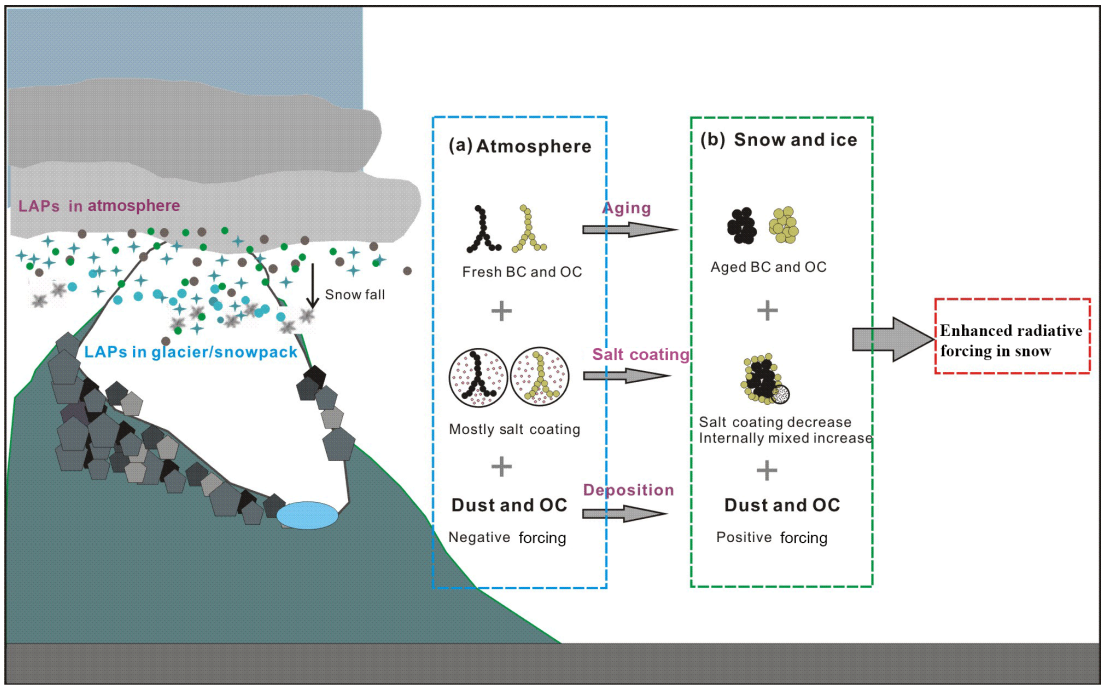

Figure 12. Schematic diagram linking aging and salt-coating change and comparing its influence to the radiative forcing between the atmosphere and snowpack of a remote glacier basin, thereby causing markedly enhanced heat absorption.

while showing positive forcing in the glacier–snowpack surface, as indicated by IPCC AR5 (2013), Yan et al. (2016), Zhang et al. (2018), and Hu et al. (2018). Thus, the light-absorbing properties of LAPs as a whole will increase greatly in glacier–snowpack surface environments.

Therefore, the great change of glacier–snowpack surface albedo may cause more strongly enhanced radiative heating than previously thought, suggesting that the warming effect from particle structure and mixing change of glacier–snowpack LAPs may have markedly affected the climate on a global scale in terms of direct forcing in the cryosphere.

4 Conclusions

The results showed that the LAP structure changed greatly in snowpack compared to that in the atmosphere, mainly due to particle aging (mainly BC and organic matter), and the salt-coating reduction process through the impurity particle's atmospheric deposition. Many more aging BC, OM, and more internally mixed BC particles were observed in the glacier–snowpack than in the atmosphere during the simultaneous observations; for example, the proportions of aged BC and OM vary from 4 % to 16 % and 12 % to 25 % in the atmosphere and from 25 % to 36 % and 36 % to 48 % in the snowpack of the cryosphere. In addition to the heat-absorbing properties from the LAP structure change above, the absorbing property of dust and OC in the atmosphere and cryosphere (snow and ice) also shows a large difference.

A schematic diagram was presented in the study and is shown in the figure, linking the explanation of the LAP structural aging and salt-coating change and comparing their influences to the radiative forcing between the atmosphere and glacier–snowpack. The LAPs in glacier–snowpack will change to more aged and internally mixed states compared to that of the atmosphere. Thus, the light absorption of the LAPs as a whole will increase greatly in glacier–snowpack environments. Moreover, we also evaluated the increase in radiative forcing caused by the particle structures and mixing state changes of LAPs. The albedo changes in MG, YG, and QG were evaluated using the SNICAR model simulation for distributed surface impurities in the observed glaciers caused by salt-coating changes, which decreased by 16.7 %–33.9 % compared to glacier surface with similar conditions to that in the atmosphere. The RF change caused by salt-coating changes varied between 1.6 and 26.3 W m^2 depending on the scenario (low, medium, or high snow density). We find that the individual particle-related albedo of the LAPs and radiative forcing change in this work is of importance in understanding the contribution of individual particle structure and mixing change in the atmosphere–snowpack interface, which may have markedly affected the climate on a global scale in terms of direct forcing in the cryosphere, and needs to be further studied in the future.

Data availability. The laboratory data set is included in Figs. 3, 5, 7, 9, and 10. Any other specific data can be provided by the authors on request.

Supplement. The supplement related to this article is available online at: https://doi.org/10.5194/tc-12-3877-2018-supplement.

Author contributions. ZD and SK designed the study, ZD and XQ collected the field samples, and ZD, DQ, YS, and SU performed laboratory measurements. All authors contributed to the discussion of the results. ZD led the writing of the paper and all co-authors contributed to it.

Competing interests. The authors declare that they have no conflict of interest.

Acknowledgements. This work was funded by the National Natural Science Foundation of China (41671062, 41721091), the State Key Laboratory of Cryosphere Sciences (SKLCS-ZZ-2018), and the Youth Innovation Promotion Association, CAS (2015347). We also thank the fieldwork team (especially to Li Kaiming, Li Gang, Li Yang and Chen Shifeng) in the northeastern Tibetan Plateau for their logistical work and sample collections. All the data used are contained within the paper and tables, figures, and references.

Edited by: Joel Savarino
Reviewed by: Marie Dumont, Jamie L. Ward, and one anonymous referee

References

Anesio, A. M., Hodson, A. J., Fritz, A., Psenner, R., and Sattler, B.: High microbial activity on glaciers: importance to the global carbon cycle, Glob. Change Biol., 15, 955–960, https://doi.org/10.1111/j.1365-2486.2008.01758.x, 2009.

Bond, T. C., Doherty, S. J., Fahey, D. W., Forster, P. M., Berntsen, T., DeAngelo, B. J., Flanner, M. G., Ghan, S., Kärcher, B., Koch, D., Kinne, S., Kondo, Y., Quinn, P. K., Sarofim, M. C., Schultz, M. G., Schulz, M.,Venkataraman, C., Zhang, H., Zhang, S., Bellouin, N., Guttikunda, S. K., Hopke, P. K., Jacobson, M. Z., Kaiser, J. W., Klimont, Z., Lohmann, U., Schwarz, J. P., Shindell, D., Storelvmo, T., Warren, S. G., and Zender, C. S.: Bounding the role of black carbon in the climate system: A scientific assessment, J. Geophys. Res.-Atmos., 118, 5380–5552, https://doi.org/10.1002/jgrd.50171, 2013.

Cappa, C. D., Onasch, T. B., Massoli, P., Worsnop, D. R., Bates, T. S., Cross, E. S., Davidovits, P., Hakala, J., Hayden, K. L., Jobson, B. T., Kolesar, K. R., Lack, D.A., Lerner, B. M., Li, S. M., Mellon, D., Nuaaman, I., Olfert, J. S., Petäjä, T., Quinn, P. K., Song, C., Subramanian, R., Williams, E. J., and Zaveri, R. A.: Radiative absorption enhancements due to the mixing state of atmospheric black carbon, Science, 337, 1078–1081, https://doi.org/10.1126/science.1223447, 2012.

Creamean, J. M., Suski, K. J., Rosenfeld, D., Cazorla, A., DeMott, P. J., Sullivan, R. C. White, A. B., Ralph, F. M., Minnis, P., Comstock, J. M., Tomlinson, J. M., and Prather, K. A.: Dust and Biological Aerosols from the Sahara and Asia Influence Precipitation in the Western U.S., Science, 339, 1572–1578, https://doi.org/10.1126/science.1227279, 2013.

Dong, Z., Qin, D., Kang, S., Liu, Y., Li, Y., Huang, J., and Qin, X.: Individual particles of cryoconite deposited on the mountain glaciers of the Tibetan Plateau: Insights into chemical composition and sources, Atmos. Environ., 138, 114–124, https://doi.org/10.1016/j.atmosenv.2016.05.020, 2016.

Dong, Z., Kang, S., Guo, J., Zhang, Q., Wang, X., and Qin, D.: Composition and mixing states of brown haze particle over the Himalayas along two transboundary south-north transects, Atmos. Environ., 156, 24–35, https://doi.org/10.1016/j.atmosenv.2017.02.029, 2017.

Dumont, M., Brun, E., Picard, G., Michou, M., Libois, Q., Petit, J. R., Geyer, M., Morin, S., and Josse B.: Contribution of light-absorbing impurities in snow to Greenland's darkening since 2009, Nat. Geosci., 7, 509–512, https://doi.org/10.1038/ngeo2180, 2014.

Flanner, M. G., Zender, C. S., Randerson, J. T., and Rasch, P. J.: Present-day climate forcing and response from black carbon in snow, J. Geophys. Res.-Atmos., 112, D11202, https://doi.org/10.1029/2006JD008003, 2007.

He, C., Liou, K.-N., Takano, Y., Zhang, R., Levy Zamora, M., Yang, P., Li, Q., and Leung, L. R.: Variation of the radiative properties during black carbon aging: theoretical and experimental intercomparison, Atmos. Chem. Phys., 15, 11967–11980, https://doi.org/10.5194/acp-15-11967-2015, 2015.

Hu, Z., Kang, S., Yan, F., Zhang, Y., Li, Y., Chen, P., Wang, K., Gao, S., and Li, C.: Dissolved organic carbon fractionation accelerates glacier-melting: A case study in the northern Tibetan Plateau, Sci. Total Environ., 627, 579–585, 2018.

IPCC: Climate Change 2013: The Physical Science Basis, Cambridge University Press, Cambridge, United Kingdom and New York, NY, USA, 1535 pp., 2013.

Jacobson, M. Z.: A physically-based treatment of elemental carbon optics: Implications for global direct forcing of aerosols, Geophys. Res. Lett., 27, 217–220, 2000.

Jacobson, M. Z.: Strong radiative heating due to the mixing state of black carbon in atmospheric aerosols, Nature, 409, 695–697, https://doi.org/10.1038/35055518, 2001.

Jacobson, M. Z.: Effects ofbiomass burning on climate, accountingfor heat and moisture fluxes, black andbrown carbon, and cloud absorptioneffects, J. Geophys. Res.-Atmos., 119, 8980–9002, https://doi.org/10.1002/2014JD021861, 2014.

Judson, A. and Doesken, N.: Density of Freshly Fallen Snow in the Central Rocky Mountains, B. Am. Meteorol. Soc., 81, 1577–1588, 2000.

Kaspari, S. D., Schwikowski, M., Gysel, M., Flanner, M. G., Kang, S., Hou, S., and Mayewski, P. A.: Recent increase in black carbon concentrations from a Mt. Everest ice core spanning 1860–2000 AD, Geophys. Res. Lett., 38, L04703, https://doi.org/10.1029/2010GL046096, 2011.

Kaspari, S., Painter, T. H., Gysel, M., Skiles, S. M., and Schwikowski, M.: Seasonal and elevational variations of black carbon and dust in snow and ice in the Solu-Khumbu, Nepal

and estimated radiative forcings, Atmos. Chem. Phys., 14, 8089–8103, https://doi.org/10.5194/acp-14-8089-2014, 2014.

Li, W. J., Shao, L. Y, Shi, Z., Chen, J., Yang, L., Yuan, Q., and Yan, C.: Mixing state and hygroscopicity of dust and haze particles before leaving Asian continent, J. Geophys. Res., 119, 1044–1059, 2014.

Li, W. J., Chen, S. R., Xu, Y. S., Guo, X. C., Sun, Y. L., Yang, X. Y., Wang, Z. F., Zhao, X. D., Chen, J. M., and Wang, W. X.: Mixing state and sources of submicron regional background aerosols in the northern Qinghai–Tibet Plateau and the influence of biomass burning, Atmos. Chem. Phys., 15, 13365–13376, https://doi.org/10.5194/acp-15-13365-2015, 2015.

Ming, J., Cachier, H., Xiao, C., Qin, D., Kang, S., Hou, S., and Xu, J.: Black carbon record based on a shallow Himalayan ice core and its climatic implications, Atmos. Chem. Phys., 8, 1343–1352, https://doi.org/10.5194/acp-8-1343-2008, 2008.

Peng, J., Hu, M., Guo, S., Du, Z., Zheng, J., Shang, D., Zamora, M. L., Zeng, L., Shao, M., Wu, Y., Zheng, J., Wang, Y., Glen, C. R. Collins, D. R., Molina, M. J., and Zhang, R.: Markedly enhanced absorption and direct radiative forcing of black carbon under polluted urban environments, P. Natl. Acad. Sci. USA, 113, 4266–4271, https://doi.org/10.1073/pnas.1602310113, 2016.

Qiu, J.: The third pole, Nature, 454, 393–396, https://doi.org/10.1038/454393a, 2008.

Qu, B., Ming, J., Kang, S.-C., Zhang, G.-S., Li, Y.-W., Li, C.-D., Zhao, S.-Y., Ji, Z.-M., and Cao, J.-J.: The decreasing albedo of the Zhadang glacier on western Nyainqentanglha and the role of light-absorbing impurities, Atmos. Chem. Phys., 14, 11117–11128, https://doi.org/10.5194/acp-14-11117-2014, 2014.

Ramanathan, V., Ramana, M., Roberts, G., Kim, D., Corrigan, C., Chung, C., and Winker, D.: Warming trends in Asia amplified by brown cloud solar absorption, Nature, 448, 575–578, 2007.

Semeniuk, T. A., Bruintjes, R. T., Salazar, V., Breed, D. W., Jensen, T. L., and Buseck, P. R.: Individual aerosol particles in ambient and updraft conditions below convective cloud bases in the Oman mountain region, J. Geophys. Res.-Atmos., 119, 2511–2528, https://doi.org/10.1002/2013JD021165, 2014.

Skiles, S. M., Flanner, M., Cook, J. M., Dumont, M., and Painter, T. H.: Radiative forcing by light-absorbing particles in snow, Nat. Clim. Change, 8, 864–971 https://doi.org/10.1038/s41558-018-0296-5, 2018.

Sjögren, B., Brandt, O., Nuth, C., Isaksson, E., Pohjola, V., Kohler, J., and Van de Wal, R. S. W.: Instruments and methods determination of firn density in ice cores using image analysis, J. Glaciol., 53, 413–419, doi:10.3189/002214307783258369, 2017.

Wang, M., Xu, B., Cao, J., Tie, X., Wang, H., Zhang, R., Qian, Y., Rasch, P. J., Zhao, S., Wu, G., Zhao, H., Joswiak, D. R., Li, J., and Xie, Y.: Carbonaceous aerosols recorded in a southeastern Tibetan glacier: analysis of temporal variations and model estimates of sources and radiative forcing, Atmos. Chem. Phys., 15, 1191–1204, https://doi.org/10.5194/acp-15-1191-2015, 2015.

Wang, X., Doherty, S., and Huang, J.: Black carbon and other light-absorbing impurities in snow across Northern China, J. Geophys. Res.-Atmos., 118, 1471–1492, https://doi.org/10.1029/2012JD018291, 2013.

Ward, J. L., Flanner, M. G., Bergin, M., Dibb, J. E., Polashenski, C. M., Soja, A. J., and Thomas, J. L.: Modeled response of Greenland snowmelt to the presence of biomass burning-based absorbing aerosols in the atmosphere and snow, J. Geophys. Res.-Atmos., 123, 6122–6141, https://doi.org/10.1029/2017JD027878, 2018.

Xu, B., Cao, J., Hansen, J., and Yao, T.: Black soot and the survival of Tibetan glaciers, P. Natl. Acad. Sci. USA, 106, 22114–22118, https://doi.org/10.1073/pnas.0910444106, 2009.

Yan, F., Kang, S., Li, C., Zhang, Y., Qin, X., Li, Y., Zhang, X., Hu, Z., Chen, P., Li, X., Qu, B., and Sillanpää, M.: Concentration, sources and light absorption characteristics of dissolved organic carbon on a medium-sized valley glacier, northern Tibetan Plateau, The Cryosphere, 10, 2611–2621, https://doi.org/10.5194/tc-10-2611-2016, 2016.

Yang, S., Xu, B., Cao, J., Zender, C. S., and Wang, M.: Climate effect of black carbon aerosol in a Tibetan Plateau glacier, Atmos. Environ., 111, 71–78, https://doi.org/10.1016/j.atmosenv.2015.03.016, 2015.

Zhang, Y., Kang, S., Cong, Z., Schmale, J., Sprenger, M., Li, C., Yang, W., Gao, T., Sillanpää, M., Li, X., Liu, Y., Chen, P., and Zhang, X.: Light-absorbing impurities enhance glacier albedo reduction in the southeastern Tibetan plateau, J. Geophys. Res.-Atmos., 122, 6915–6933, https://doi.org/10.1002/2016JD026397, 2017.

Zhang, Y., Kang, S., Sprenger, M., Cong, Z., Gao, T., Li, C., Tao, S., Li, X., Zhong, X., Xu, M., Meng, W., Neupane, B., Qin, X., and Sillanpää, M.: Black carbon and mineral dust in snow cover on the Tibetan Plateau, The Cryosphere, 12, 413–431, https://doi.org/10.5194/tc-12-413-2018, 2018.